Journal of Materials Chemistry B

RSC Publishing

PAPER

X-ray-amorphous calcium phosphate (ACP) synthesis in a simple biomineralization medium

Cite this: *J. Mater. Chem. B*, 2013, **1**, 4511

A. Cuneyt Tas*

Received 15th June 2013
Accepted 9th July 2013

DOI: 10.1039/c3tb20854k

www.rsc.org/MaterialsB

An inorganic solution similar to the inorganic electrolyte compartment of the DMEM (Dulbecco's modified Eagle's medium) cell culture medium is developed. This biomineralization medium contains 44.05 mM HCO_3^-, 126.86 mM Na^+, 93.37 mM Cl^-, 5.33 mM K^+, 2.26 mM Ca^{2+}, 0.905 mM $H_2PO_4^-$, and 0.81 mM Mg^{2+}. Its Ca/P molar ratio is set to be identical to that of human blood plasma, *i.e.*, 2.50. The medium is free of any Tris or Hepes but maintains a pH of 7.45 both at 37 and 65 °C. The first novelty of this solution is that it has the unique ability to homogeneously coat X-ray-amorphous calcium phosphate (ACP) on glass slides vertically immersed in it and kept at 37 °C for less than 48 h. The second innovative aspect of this solution is that it has the unprecedented ability to produce monodisperse ACP nanospheres with diameters less than 180 nm when simply heated at 65 °C for 1 h while being stirred. The third novelty of this solution is that it only forms ACP and it does not form apatite in stark contrast to many other synthetic calcification or biomineralization media known. Samples were characterized by X-ray diffraction, energy-dispersive X-ray spectroscopy, Fourier-transform infrared spectroscopy, BET surface area, contact angle goniometry, field emission-scanning and transmission electron microscopy analyses.

1 Introduction

The nucleation of crystalline calcium phosphates in aqueous solutions is occasionally preceded by the formation of amorphous calcium phosphate (ACP).[1–6] Abbona and Baronnet,[7] Brecevic *et al.*,[8] and Christoffersen *et al.*[9] were among the first to report such early-forming (*i.e.*, within the first few minutes of synthesis) ACP nanoparticles by electron microscopy. If such ACP nanoparticles were not intentionally stabilized by adding Mg^{2+}, pyrophosphate or carbonate ions[10] to the synthesis media, then they transform into crystalline octacalcium phosphate (OCP, $Ca_8(HPO_4)_2(PO_4)_4\cdot 5H_2O$) or non-stoichiometric apatitic calcium phosphate with an increase in aging time, even in their native precipitation solutions.[11–19]

ACP is a high solubility calcium phosphate phase, which is more soluble, at pH 6 to 7, than stoichiometric hydroxyapatite (HA, $Ca_{10}(PO_4)_6(OH)_2$), α-tricalcium phosphate (α-TCP, α-$Ca_3(PO_4)_2$), β-tricalcium phosphate (β-$Ca_3(PO_4)_2$) and tetracalcium phosphate (TTCP, $Ca_4(PO_4)_2O$).[20] The most common method of ACP powder synthesis by the simultaneous use of ACP stabilizers in synthesis solutions, such as Mg^{2+}, $P_2O_7^{4-}$ and HCO_3^- ions, was disclosed by Lee *et al.*[21] in relation to the industrial-scale production of ACP powders for a specific bone cement formulation. This patented procedure is comprised of rapidly adding a solution of Ca-nitrate tetrahydrate (100 mM) and Mg-chloride hexahydrate (2.7 mM) to a highly alkaline solution containing sodium hydroxide (700 mM), disodium hydrogen phosphate (115 mM), sodium bicarbonate (200 mM) and sodium pyrophosphate (2.5 mM) under vigorous stirring at room temperature.[21] If one removes the pyrophosphate and Mg ions (ACP stabilizers) and the excessive sodium hydroxide from the synthesis recipe of Lee *et al.*,[21,22] the resultant solids would only be cryptocrystalline (*i.e.*, poorly crystalline) calcium phosphate but not X-ray-amorphous at all.[23]

The aforementioned synthesis procedure, which is devoid of any organic additives, consisted of two-steps, involving the preparation of two separate solutions and their rapid mixing with one another. Furthermore, if the calcium ions were in one solution and the protonated phosphate (HPO_4^{2-}) ions were in another solution as in the procedure of Lee *et al.*,[21,22] then such "strike precipitation" processes would not produce ACP precipitates with well-defined geometrical shapes, such as spheres. The characteristic non-spherical ACP precipitates of these two-step processes look quite similar in particle morphology to those reported in 1977 by Eanes and Meyer.[24] We suggest the readers to examine the hydrated, feather-like aggregated particles depicted in Fig. 11 of ref. 24.

To the best of our knowledge, the literature for the one-pot, single step synthesis of submicron- or nano-spheres of ACP, especially in the absence of any organic additives, is difficult to come by.[10,25] Synthesizing ACP powders from an initially precipitate-free, single solution (also free of any organic substances which are not present in the human metabolism) at the physiological pH (7.4) still remains a challenge. The goal of

Dept. of Materials Science and Engineering, University of Illinois, Urbana 61801, USA. E-mail: c_tas@hotmail.com; Web: http://www.cuneyttas.com; Fax: +1 217 333 2736; Tel: +1 217 344 6708

the current study is to develop a single solution and a simple process which shall *in situ* produce submicron- or nano-spheres of ACP upon heating that solution from room temperature to a moderate temperature, such as 65 °C, in glass reactors.

In developing such a solution, one starts by noting that Mg^{2+} (at 1.5 mM) and HCO_3^- (at 27 mM) ions, both being strong ACP stabilizers,[10,25] are present in human blood plasma. The current author was the first to develop a biomimetic process using a Tris-buffered SBF (synthetic body fluid) solution containing 27 mM HCO_3^- (*i.e.*, the exact bicarbonate concentration of blood plasma) and 1.5 mM Mg^{2+} to synthesize amorphous calcium phosphate (ACP) powders consisting of 20–30 nm particles (with a BET surface area >160 $m^2\ g^{-1}$) in that solution[26–28] at 37 °C and pH 7.4. However, that SBF solution contained Tris (*tris-hydroxymethyl-aminomethane, $(HOCH_2)_3CNH_2$*) to fix the pH at 7.4. Tris is not present at all in the human metabolism. The goal of the current study is to synthesize nanospheres of ACP in a solution which is free of Tris but still has a pH of 7.4. Barrere *et al.*,[29] in a follow-up to our studies,[26,27] showed that multiplying the HCO_3^- concentration of the severely HCO_3^--deficient Kokubo SBF (*i.e.*, only 4.2 mM)[30,31] by a factor of 5 (to attain 21 mM; still significantly short of the 27 mM level of the blood plasma) would produce ACP precipitates instead of cryptocrystalline apatitic calcium phosphate.

To provide a historical perspective, Earle's balanced salt solution (EBSS),[32] developed in 1943, is one of the first synthetic biomineralization media (although at the time of their development, researchers did not see such solutions as a versatile milieu to perform *in vitro* biomineralization and biomimetic synthesis studies) to mimic the ion concentrations of blood plasma without using any Tris or Hepes (*2-(4-(2-hydroxyethyl)-1-piperazinyl)ethane sulphonic acid, $C_8H_{18}N_2O_4S$*). Hepes, like Tris, is also not present in human blood. EBSS had a HCO_3^- (bicarbonate ion) concentration of 26.2 mM (close to that of human blood, 27 mM) and a Ca/P molar ratio of 1.8 (in stark contrast to that of human blood, which is 2.50). The pH value (7.4) of EBSS is identical to that of blood.

Hanks' balanced salt solution (HBSS),[33] developed in 1949, was again a medium free of any Tris of Hepes, but quite deficient in its HCO_3^- concentration (4.2 mM) and Ca/P molar ratio (1.6) in comparison with those of blood. Tyrode solution, with a Ca/P molar ratio of 4.5 and a HCO_3^- concentration of 12 mM, is a Tris- or Hepes-free basal salt medium.[34] Krebs–Ringer bicarbonate buffer (KRBB),[35] developed in 1932, is a Tris/Hepes-free solution which raises the HCO_3^- concentration of the Ringer solution[36] from zero to 27 mM, *i.e.*, to that of blood plasma.

Solution formulations commonly used in the culturing of mammalian cells were the major inspiration points for the current study. Cell culture solutions, which were developed decades before the Kokubo SBF,[30,31] contain Ca^{2+}, Mg^{2+}, Na^+, K^+, HPO_4^{2-}, Cl^- and HCO_3^- ions in concentrations similar to those found in blood plasma. A recent article by Boccaccini *et al.*[37] disclosed that the Tris-buffer present in the SBF (simulated/synthetic body fluid) solutions[30,31] was causing an increased dissolution of the surface constituents of bioglass and glass-ceramic samples soaked in it and therefore led to the premature crystallization of apatite on sample surfaces, tarnishing the reliability of those so-called *in vitro* bioactivity measurements based on such SBF solutions. Tris is known to be a calcium chelator.[38]

Dulbecco's modified Eagle's medium (DMEM), for instance, is a commercially available medium widely used for cell culture supporting the growth of mammalian cells, and its formulation is inspired by the Eagle's minimum essential medium.[39–41] DMEM solutions (Ca/P molar ratio = 1.99) possess a number of amino acids, vitamins, inorganic salts and can be obtained either in liquid or powder form, also with or without Hepes buffer and phenol red. DMEM solutions contain 44 mM HCO_3^-, the highest concentration of bicarbonate ions among any such media. The original Eagle's minimum essential medium formulation, on the other hand, had a HCO_3^- concentration of 23.8 mM.[39,40]

We previously reported the complete transformation of brushite (DCPD, dicalcium phosphate dihydrate, $CaHPO_4 \cdot 2H_2O$) powders in less than a week to octacalcium phosphate (OCP), but not to apatitic calcium phosphate, when a commercial DMEM solution was used as the soak test medium at 37 °C.[42] The removal of all the amino acids, vitamins, glucose/dextrose, phenol red, Hepes and pyruvate from the DMEM formulation and raising the Ca/P molar ratio of the thus modified form of biomineralization solution from 1.99 to 2.50 led to a much faster transformation of DCPD powders to OCP in comparison with DMEM.[43]

We hereby report a newly discovered ability of an easy-to-prepare, initially precipitate-free, Tris- or Hepes-free solution we formulated, with a HCO_3^- concentration of 44 mM, a pH of 7.4, and a Ca/P molar ratio of 2.50,

(i) to form submicron spheres of X-ray-amorphous calcium phosphate in powder form only upon heating the solution to 65 °C or

(ii) to *in situ* deposit spherulites of ACP (at 37 °C) on ordinary glass slides immersed in them.

2 Experimental

2.1 Materials and solution preparation

Calcium chloride dihydrate (>99.5%, $CaCl_2 \cdot 2H_2O$, Fisher Scientific, Catalog no: C79), magnesium chloride hexahydrate (>99.5%, $MgCl_2 \cdot 6H_2O$, Fisher, no: AC19753), potassium chloride (>99.5%, KCl, Sigma, no: P3911), sodium hydrogen carbonate (>99.9%, $NaHCO_3$, Merck, no: 106329), sodium chloride (>99.8%, NaCl, Merck, no: 106404), and sodium dihydrogen phosphate monohydrate (>99.9%, $NaH_2PO_4 \cdot H_2O$, EMD Chemicals, no: SX07101) were used in solution preparation. One may also use NaH_2PO_4 if $NaH_2PO_4 \cdot H_2O$ is unavailable. The use of anhydrous $CaCl_2$, in place of $CaCl_2 \cdot 2H_2O$, is not recommended since it is a highly hygroscopic substance and may cause inaccurate Ca^{2+} concentrations in the resultant solutions. Freshly boiled (to remove any dissolved bicarbonate ions originating from the prolonged contact of the water reservoir with laboratory atmosphere) de-ionized water (18.2 MΩ) was used in all experiments.

One liter of the new biomineralization medium of this study was prepared by adding the indicated amounts of chemicals in Table 1, in the order given, to 998 mL of pre-boiled deionized

Table 1 Biomineralization medium preparation (*1 liter*)

Chemical	Amount g L^{-1}	Ion	Concentration mM
NaCl	4.7865	Na^+	126.86
KCl	0.3974	K^+	5.33
$MgCl_2 \cdot 6H_2O$	0.1655	Mg^{2+}	0.81
$CaCl_2 \cdot 2H_2O$	0.3323	HCO_3^-	44.05
$NaHCO_3$	3.7005	Cl^-	93.37
$NaH_2PO_4 \cdot H_2O$	0.1250	Ca^{2+}	2.26
		$H_2PO_4^-$	0.905

Table 2 Compositions of media mentioned or developed in this study (*ions in mM*)[a]

	Na^+	K^+	Mg^{2+}	Ca^{2+}	P	HCO_3^-	Cl^-	SO_4^{2-}
Plasma	142	5	1.5	2.5	1	27	103	0.5
SBF[53]	142	5	1.5	2.5	1	27	103	0.5
Ringer[36]	113.6	1.88	—	1.08	—	2.38	115.3	—
HBSS[33]	141.6	5.81	0.81	1.26	0.78	4.07	144.8	0.81
Tyrode[34]	149.1	2.7	0.53	1.8	0.33	11.9	144	—
EBSS[32]	143.4	5.36	0.83	1.8	1.04	26.2	125.3	0.83
KRBB[35]	143.4	5.88	1.25	2.52	1.18	25	128.2	1.25
DMEM[42]	127	5.33	0.81	1.80	0.905	44.05	90.8	—
This study	127	5.33	0.81	2.26	0.905	44.05	93.4	—

[a] Note: DMEM solutions also contain amino acids, vitamins and glucose.

water. The as-prepared solutions had a pH value (7.45 ± 0.05 at both room temperature, 22 ± 1 °C, and 65 ± 0.3 °C) similar to that of blood plasma. ACP powder syntheses were performed in heat-sterilized (130 °C, 8 h) and unused Pyrex® glass media bottles. Inorganic ion concentrations shown in Table 1 strictly mimic those of the DMEM solutions with the only exception of Ca^{2+}. The calcium concentration of the original DMEM solution was intentionally increased in this study from 1.80 to 2.26 mM to attain a Ca/P molar ratio of 2.50 (*i.e.*, that of human blood) in the biomineralization medium. The solutions were stored in clean and sealed glass bottles in a refrigerator (+4 °C) when not in use.

The ion concentrations of the solution of this study (Table 1) are compared in Table 2 with other solutions mentioned in the previous section.

2.2 ACP coating on glass

ACP formation on ordinary optical microscope slide glasses was achieved by vertically inserting a slide (Fisher Scientific, 60 × 20 × 1 mm) into a glass media bottle (100 mL capacity) containing 100 mL of the solution of Table 1. The bottle containing the vertically-placed glass slide was kept undisturbed in an oven at 37 °C for 48 h. The glass slide was then washed with 500 mL of deionized water and dried at RT for 36 h in air.

2.3 ACP powder synthesis

Any desired volume of the solution described in Table 1 was placed in a Pyrex® glass media bottle of suitable capacity. The screw-capped bottle (with a thermometer attached to a hole in its plastic cap) was placed on a hot-plate and heated to 65 ± 1 °C for about 20–25 minutes and the solution in it was constantly stirred at 750 rpm using a magnetic stir bar (1 cm diameter and 5 cm long stir bar used in a 500 mL bottle). The total heating time at the constant temperature of 65 °C was 60 minutes. The first ten minutes of that 60 min was the incubation time, in which the solution did not exhibit any visible turbidity. At around the 10th minute at 65 °C, the solution first displayed a bluish tint (the onset of ACP nanosphere formation) for a short while (typically 15–20 seconds) and then rapidly went turbid and milky. The synthesis procedure is this simple. The resultant fine particles were separated from their mother solution by centrifugation at 10 000 rpm or by filtering through a 0.22 μm filter membrane and then washed with 1 L of deionized water, followed by drying for 36 h at RT in air.

2.4 Sample characterization

Prior to powder X-ray diffraction (XRD) and Fourier-transform infrared spectroscopy (FTIR) analyses, the dried samples were manually ground in an agate mortar using an agate pestle. XRD runs were performed (Advance D8, Bruker, Karlsruhe, Germany and Ultima IV, Rigaku, Tokyo, Japan) in the step scan mode, with a step size of 0.03° and a preset time of 3 seconds. The powder diffractometers were equipped with Cu tubes and operated at 40 kV and 40 mA. XRD powder samples were prepared by gently packing the powders into single-crystal quartz sample holders with a cavity of around 1 mm deep. ACP-coated glass samples were X-rayed *as is*.

The wettability of ACP-coated glass slides (*versus as is* glass slides) was determined using an OCA 15 Plus (DataPhysics Instruments, Filderstadt, Germany) contact angle goniometer *via* the static sessile drop method (3 μL drop volume) with deionized water at RT. The contact angle goniometer photographs, which served as the sole comparison tool for wettability differences in the specimens of this study, were originally captured as a 15 minutes continuous movie at the rate of 25 frames per second (fps).

FTIR samples were mixed with KBr powders at the ratio of 1 mg sample-to-250 mg KBr in an agate mortar. FTIR pellets with a diameter of 12.5 mm were pressed at a load of 10 tons applied for 1 min. FTIR data were collected (Spectrum One, PerkinElmer, Waltham, MA) using 256 scans at 2 cm^{-1} resolution.

Samples for field emission-scanning electron microscopy (FE-SEM) and energy-dispersive X-ray spectroscopy (Zeiss-Neon 40 EsB, Oberkochen, Germany) were not ground and small portions of the samples embedded on conducting carbon tapes were sputter-coated with a thin (approx. 5 nm thick) layer of gold-palladium prior to imaging at 5 kV at a working distance of 6 mm. Transmission electron microscopy (JEOL 2010F, Tokyo, Japan) was performed at 200 kV to analyze the ACP powders, after placing a tiny drop of ethyl alcohol suspension of the powders onto a Cu grid. Quantitative chemical analyses of the powder samples were performed by inductively-coupled plasma atomic emission spectroscopy (ICP-AES, Model 61E, Thermo Electron, Madison, WI). For the ICP-AES analyses, 75 mg

portions of the powder samples were dissolved in 5 mL of concentrated HNO_3 solution.

The BET surface area of the powder samples was determined by applying the standard Brunauer–Emmett–Teller method to the nitrogen adsorption isotherm obtained at −196 °C using a Quantachrome, Nova 2000e (Boynton Beach, FL) instrument.

3 Results

3.1 Coating on glass

Glass slides vertically immersed in the biomineralization media (at 37 °C) similar to amino acids-, vitamins-, Hepes-, glucose/dextrose-, pyruvate-free DMEM solution were covered with a monolayer of calcium phosphate visible to the naked eye in 48 h (Fig. 1a). Glass slides kept in the solutions for only 24 h (data not shown) were also covered with CaP (calcium phosphate) but the surface coverage was not as complete as those of the 48 h samples. X-ray diffraction (XRD) analyses showed that the deposited CaP was X-ray-amorphous (Fig. 1b). The large hump (from 10 to 40° 2θ) seen in Fig. 1b was due to the base silicate glass. Solution-precipitated CaPs (such as those obtained in SBF solutions) typically exhibit moderately high intensity X-ray peaks at 25.89° and at 31.78 to 34.05° 2θ, and such apatitic CaP peaks were absent in Fig. 1b.

Field emission-scanning electron microscope (FE-SEM) photomicrographs of glass slides vertically immersed in the solution for 48 h at 37 °C given in Fig. 1c and d, at increasing magnifications, displayed the extent of surface coverage. The high resolution image of Fig. 1d depicted that the ACP deposits covering the glass slide surface were actually comprised of aggregates of approximately 20 nm spheroidal particles. Fig. 1e shows the surface of a similar ACP-coated glass slide (but without any Au/Pd sputter-coating) taken at the same magnification with that of Fig. 1d. Therefore, those 20 nm spheroidal particles are not an artifact of sputter-coating. Both Fig. 1d and e provide some evidence that the vacuum in sputter coating causes the formation of microcracks on the ACP layer deposited on glass slides. The qualitative energy-dispersive X-ray spectroscopy (EDXS) data of the ACP-coated glass slides were quite similar to those depicted later in Fig. 3b and the deposited layer contained Ca, P and Mg. The monolayer of ACP deposited on glass slides was about 200 nm thick (Fig. 1c).

The *as is* glass slides were not hydrophilic at all, however, the ACP-coated glass slides displayed a significant wettability as shown in the contact angle goniometry data of Fig. 2. The *as is* glass sample (with an initial contact angle of about 51–53°) is shown in the left column of Fig. 2, as a function of the elapsed time (in seconds) upon the contact of the sessile drop with the

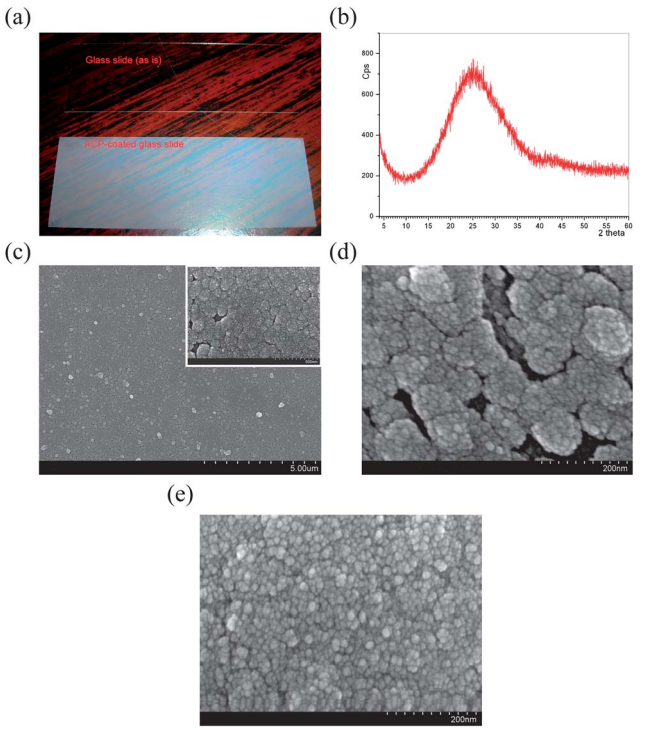

Fig. 1 (a) Digital camera photo, (b) characteristic XRD spectrum, (c) & (d) low and high resolution FE-SEM images of ACP-coated glass slides (with Au/Pd sputter-coating) upon vertical immersion in the solution of Table 1 at 37 °C for 48 h, (e) FE-SEM image of an ACP-coated glass slide similar to that depicted in (d) but without any Au/Pd sputter-coating.

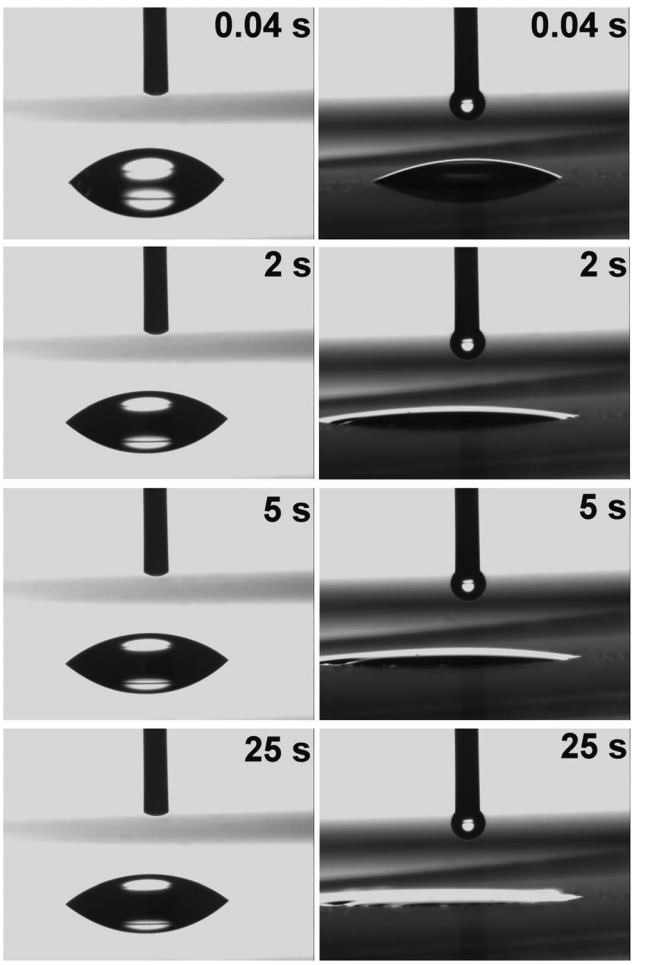

Fig. 2 Contact angle goniometry images of a static sessile drop on glass slides, left column: *as is* glass; right column: ACP-coated glass (still photos extracted from a 15 min movie recorded at 25 fps, *image labels = elapsed seconds after the drop touched the surface*).

surface. The contact angle of the *as is* glass sample did not change noticeably with the elapsed time. The ACP-coated glass slide is shown in the right column of Fig. 2, and the initial contact angle was around 26–28°. The apparent contact angle of the ACP-coated glass sample dropped to 11° after 2 s and to about 2° after 25 s (Fig. 2). The initial drop had the tendency to spread on the ACP-coated glass surface. Contact angle on a surface is defined by the Young equation and the shape of a drop resting on a surface depends on the material properties of the drop, the atmosphere surrounding it, and most importantly the surface on which it was placed.[44] In light of the contact angle goniometry data given in Fig. 2, the simple solution technique described here seemed to be effective in turning a hydrophobic surface into a surface of remarkable wettability, and the investigation of the applicability of this solution technique to hydrophobic biopolymer and bioceramic surfaces warrants further research.

3.2 Powder synthesis

The powders synthesized by simply heating the biomineralization solution at 65 °C for 1 h were found to be X-ray-amorphous (Fig. 3a). The EDXS data of the powders showed that they were Mg-doped ACP (Fig. 3b). ICP-AES analyses were performed on three different powders separately synthesized three times using the same procedure. The amounts of magnesium in the powders were found to be 0.16, 0.14 and 0.17 wt% in these ICP-AES runs. Na, K, and Cl contents of the powders were both below the 80 ppm blank level. On the other hand, Ca/P molar ratios of the same powders were determined to be 1.30, 1.34 and 1.29 along the same ICP-AES runs used to determine the above Mg contents. We opted to report these numbers separately since reporting the average values might have hidden the slight batch-to-batch variations in those. The Ca/P molar ratios of the powders of this study agreed well with those reported by Christoffersen *et al.*[45] The current study unfortunately lacked any quantitative C analyses to determine the carbonate content of powders.

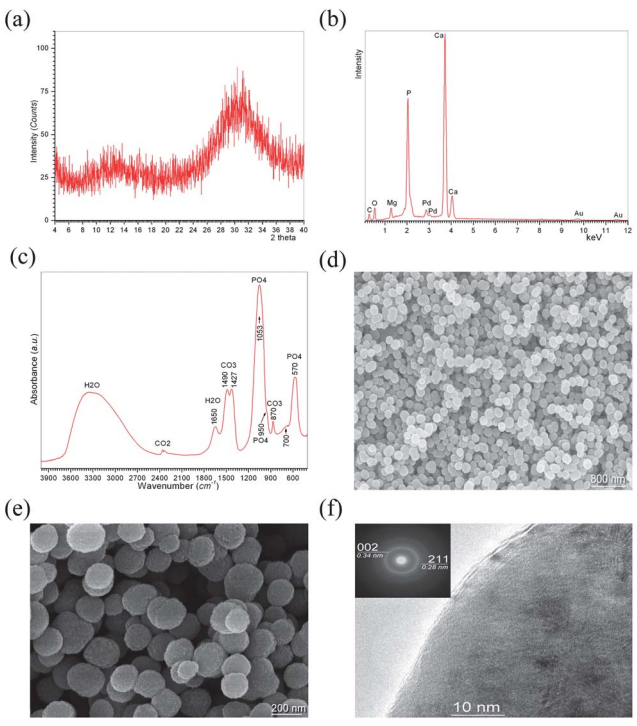

Fig. 3 ACP nanospheres synthesized in the solution of Table 1 upon heating the solution at 65 °C for 1 h; (a) XRD, (b) EDXS, (c) FTIR, (d) & (e) low and high resolution FE-SEM images, (f) TEM image and SAED pattern.

Fig. 3c shows the characteristic FTIR spectra of these powders. The samples were carbonated, as indicated by the strong bands observed at 1490–1427 and 869 cm^{-1}. The bands for the P–O vibrations of the orthophosphate group are similar to those previously observed for amorphous calcium phosphates,[46] and are found at 1053, 950 and 570 cm^{-1}. Further confirmation of the X-ray-amorphous nature of these samples came from the single broad band at around 570 cm^{-1}.[25] The band at 700 cm^{-1} should not be confused with that of the $P_2O_7^{4-}$ group usually seen from 727 to 740 cm^{-1}. The strong bands of water vibrations at 3350 and 1650 cm^{-1} prove the hydrated nature of these samples. The complete IR band assignments to ACP samples are reported elsewhere.[10,25,27,47]

The X-ray-amorphous powders obtained by heating the biomineralization solution at 65 °C for 1 h were comprised of spheres with diameters ranging from 105 to 195 nm, as shown in the SEM photomicrographs given in Fig. 3d and e. The average particle diameter was determined to be 176 ± 29 nm, which was calculated using the Heyn's lineal intercept method (in accord with ASTM standard E112-10)[48] based on the results of 60 measurements on the image given in Fig. 3d. The BET (Brunauer–Emmett–Teller) surface areas of the powders of Fig. 3d and e were 186, 183, and 189 $m^2\ g^{-1}$ for three different samples obtained from three reproduction syntheses. The 176 nm spheres of the powders were similar to the ACP deposited on glass slides at 37 °C (*i.e.*, Fig. 1c and d) and they were comprised of aggregates of smaller spheroids with the mean diameter of about 20 nm (Fig. 3e).

The TEM study performed on the powders, which were synthesized by heating the biomineralization solution at 65 °C for 1 h, depicted that the imaged nanospheres cannot be named as completely amorphous (Fig. 3f). While the image of Fig. 3f itself showed short-range order confined to discrete nanodomains only, the SAED (*selected-area electron diffraction*) pattern in its inset exhibited weak and incompletely presented diffraction spots which can be indexed with the (002) and (211) reflections of Ca-deficient, carbonated apatitic calcium phosphate. One may also consider freeze-drying the ACP precipitates immediately after removing them from their mother liquor in contrast to our RT-drying procedure. Amorphous, and hydrated, substances would pose the risk of partially transforming into cryptocrystalline materials while analyzing them using a 200 kV TEM electron beam. Nevertheless, it is a well-known fact that indisputably amorphous materials can only be produced by rapidly quenching a molten substance from elevated temperatures.

4 Discussion

The experiments of this study which were presented above under two categories; (i) static (*i.e.*, no stirring) coating on

vertically positioned glass slides at 37 °C over time periods measured in days and (ii) rapid (measured in minutes) precipitation from an agitated, stirred solution at 65 °C, actually correspond to the two facets of the same thermodynamic phase separation phenomenon: thermal decomposition of the solution given in Table 1. This solution does not precipitate any ACP or cryptocrystalline apatitic CaP as long as it is kept refrigerated at 4 °C. However, if it is kept in a sealed glass bottle in a warm and non-cooled room (*e.g.*, during the summer months) whose temperature may readily exceed 30 °C, it *in situ* precipitates ACP. This observation became the starting point for this research.

4.1 Solution chemistry

Posner clusters (*i.e.*, $Ca_9(PO_4)_6$), with sizes close to 0.8 nm, are present in supersaturated and metastable CaP solutions claimed to simulate the electrolyte portion of blood plasma, as experimentally proved by Oyane *et al.* using dynamic light scattering.[49] Directly quoting from the work of Posner,[50,51] in the process of ACP formation in solution, $Ca_9(PO_4)_6$ clusters form first (with the experimental support to this provided by the later work of Oyane *et al.*[49]) and then are aggregated randomly to produce the larger spherical particles with the inter-cluster space filled with water. The solution of Table 1 should have similar Posner clusters prior to its *in situ* precipitation of ACP when it is warmed up.

The solution of Table 1, being similar to the inorganic electrolyte portion of a DMEM cell culture medium, has a high ionic strength associated with a HCO_3^- concentration 1.632 times that of human blood plasma. The ionic strength of the solution of this study (*i.e.*, 141.4 mM) is calculated using the below formula.

$$I = \tfrac{1}{2}[(2.26\times10^{-3})(2)^2 + (126.86\times10^{-3})(1)^2 + (0.905\times10^{-3})(1)^2 + (93.37\times10^{-3})(1)^2 + (44.05\times10^{-3})(1)^2 + (5.33\times10^{-3})(1)^2 + (0.81\times10^{-3})(2)^2] = 0.1414\ \text{M} = 141.4\ \text{mM} \quad (1)$$

(Ca^{2+}, Na^+, $H_2PO_4^-$, Cl^-, HCO_3^-, K^+, Mg^{2+})

On the other hand, the ionic strength of the inorganic electrolyte portion of human blood plasma is 149.5 mM and this ionic strength value is strictly observed in designing and preparing, for instance, biomimetic SBF solutions buffered using the pair of Na-lactate and lactic acid.[52,53] The solution of Table 1 has lower Mg^{2+}, Ca^{2+}, Na^+, Cl^- and phosphate concentrations in comparison with blood plasma. Similarly, this solution's HCO_3^- concentration is much higher than that of blood plasma, as mentioned above, and HCO_3^- is a stabilizer of ACP. The low NaCl and high bicarbonate amount of this solution, which is similar to DMEM, is the reason why it does not lead to apatite precipitation. The ACP-stabilizing power of the solution of Table 1 resulted from its high HCO_3^- concentration and lower amounts of other ions.

It is a routine practice to bring the distilled/deionized water, which will later be used in a synthesis reaction, to a rolling boil for a few minutes to drive off any dissolved bicarbonate ions from water in the form of CO_2 gas. The same procedure was practiced for water used in this study to ensure the attainment of the correct HCO_3^- concentration stated in Table 1. The merit of heating/boiling of water is explained by the below reactions. It is not even necessary to boil the water to drive these reactions; warm water in comparison with cold water will allow these degassing reactions to proceed faster. To draw an analogy with the large-scale meaning of the below reactions, some environmental agencies are continuously monitoring the sea surface temperatures (SST), especially over the equatorial oceans which contain vast reserves of HCO_3^-(aq.)[54]

$$HCO_3^-(aq.) + H^+(aq.) \rightarrow CO_2(aq.) + H_2O \quad (2a)$$

$$CO_2(aq.) \rightarrow CO_2(g). \quad (2b)$$

In biology, on the other hand, CO_2 is a key metabolite in all living organisms and it exists in equilibrium with HCO_3^-. The enzyme carbonic anhydrase regulates the completely reversible reaction (2a) between aqueous HCO_3^- and dissolved CO_2.[55]

4.2 Formation of nanospheres

The role of eqn (2a) and (2b) on the formation of those 20 nm diameter fundamental (*i.e.*, building block) nanospheroids/nanospheres, which then aggregate to form the larger ones, depicted in the high magnification FE-SEM image of Fig. 1d and 1e (and partly in Fig. 3e) is crucial to determine. It might be unrealistic to think that in a solution heated to 65 °C, the initial HCO_3^- concentration would still remain unchanged. Posner clusters of 0.8 nm diameter are present in a precipitate-free CaP solution,[49,56] their inter-cluster space is filled with the electrolyte solution,[51] and the degassing eqn (2a) and (2b) become operational exactly in that inter-cluster liquid with an increase in the temperature of the solution. Did an increase in the solution temperature from RT to 37° or from RT to 65 °C cause an increase in the sizes of those fundamental nanospheroids? The common size (*i.e.*, 20 nm) acquired by those shown both in Fig. 1d (37 °C) and Fig. 3e (65 °C) is noteworthy in asserting that this size seemed to be temperature-independent.

Yin and Stott[56] postulated that a Posner cluster is bound by 6 protons (H^+) and, therefore, is a positively charged entity. To maintain local charge neutrality, it will be reasonable to assume that the positively-charged Posner clusters are surrounded by negatively-charged bicarbonate and hydroxyl ions (also with Cl^-) in a supersaturated and metastable solution such as the solution of Table 1 of this study. This coordination shall persist until the 10^{th} minute of the incubation period during which no turbidity or

tint in the solution is observed. However, if and when eqn (2a) becomes operational, a significant fraction of the coordinating bicarbonate ions may be gradually eliminated while taking some of the H^+ away with them (*i.e.*, deprotonation) and leaving the OH^- and Cl^- behind. This may represent the moment of transition from Posner clusters to Ca-deficient apatitic CaP nanodomains shown in the TEM image of Fig. 3f. Moreover, when eqn (2b) becomes operational simultaneously with eqn (2a); and if microscopic bubbles of CO_2(g) start forming in the inter-cluster spaces of Posner clusters, then those newly created local liquid–gas interfaces may act as the preferential sites for the heterogeneous nucleation of those 20 nm-diameter fundamental nanospheroids (of Fig. 1d and 1e). We are fully aware that such speculations need to be confirmed by experimental observations, albeit this is difficult to achieve with the current level of *in situ* microscopic imaging technology pertinent to aqueous solutions at the nanoscale.

4.3 Influence of Mg^{2+} and HCO_3^-

If one prepares a new solution similar to that of Table 1, without any $NaHCO_3$ addition, this solution mainly precipitates brushite ($CaHPO_4 \cdot 2H_2O$) upon its heating to 37 °C. Likewise, if one prepares another solution similar to that of Table 1, without any $MgCl_2 \cdot 6H_2O$ but with $NaHCO_3$, the new solution precipitates cryptocrystalline (*i.e.*, poorly crystalline) apatitic calcium phosphate, but not X-ray-amorphous CaP upon heating to 37 °C. These are experimental observations based on our previous studies related to biomineralization media development.[26,27,43,53] Therefore, there seem to be two key constituents of the solution of Table 1: (1) HCO_3^- (aq.), (2) Mg^{2+} (aq.) to impart it the ability to produce ACP nanospheres, instead of cryptocrystalline apatitic CaP, upon simple heating. These two constituents, being effective ACP stabilizers,[57] at their stated concentrations, apparently ensured the formation of ACP nanospheres with mean sizes less than 180 nm.

Nevertheless, to complicate the matters further, this does not mean that any saline solution containing Mg^{2+} and HCO_3^- at any concentration can form ACP nanospheres within this size range. Dorozhkin *et al.*[58] tested the influence of Mg^{2+} and HCO_3^- in SBF-like solutions at 4, 8 and 16 times above the normal concentrations, however, the resultant powders consisted only of cryptocrystalline apatitic CaP.

Zhou and Bhaduri[59] were able to form spheres of CaP over the diametrical size range of 250 to 450 nm but they were not able produce single phase ACP. Their samples were contaminated with unidentified phase(s) of significant crystallinity as confirmed by their XRD data, although they increased the Mg^{2+} concentration of their SBF-like solutions to 8 or 24 times that of the human blood plasma. Zhou and Bhaduri[59] were only forming cryptocrystalline apatitic CaP (with XRD peaks at 25.89° and at 31.78 to 34.05° 2θ) when they kept the Mg^{2+} concentration of their solutions at the level of blood plasma. In contrast to the above, the solution of Table 1, similar to DMEM but devoid of amino acids, vitamins, and their like, has its Mg^{2+} concentration fixed at about half that of the blood plasma. In other words, the solution of this study did not necessitate an increased Mg^{2+} content in order to suppress the formation of cryptocrystalline apatitic CaP.

4.4 Similarity of ACP nanospheres to those seen in bone tissue

It is relatively easy for materials scientists to synthesize spheres of CaP in laboratory glassware. The main question here is: do these *in vitro* globules/spheres resemble the morphology of the calcospherites of bone tissue during biological bone remodeling *in vivo*? The answer to this question is positive and an amazingly strong evidence for such resemblance is given in Fig. 10 and 11 of the article by Sela.[60] The readers are advised to compare those SEM images[60] with the SEM photomicrographs presented in this study. Moreover, submicron spherical ACP particles were found in the teeth of chitons.[61] ACP is known to first transform into OCP and then into cryptocrystalline apatitic CaP during its maturation in biological fluids, such as blood, urine, saliva and milk.[62]

4.5 Addition of gelatin to the biomineralization media

The addition of organics into inorganic synthesis solutions are known to alter the size and shape distribution of precipitates obtained. The influence of water soluble bovine gelatin (which is a balanced concoction of amino acids[63]) added (at levels from 1 to 1120 mg L^{-1}) to equimolar solutions (free of K^+, Mg^{2+}, and HCO_3^-) of calcium chloride and sodium phosphate (6 mM each) on the mean particle size of synthesized ACP particles was previously studied by Brecevic *et al.*[8] They reported that at gelatin additions above 400 mg L^{-1}, the ACP particles became monodisperse with diameters around 100 nm. Based on this previous study, we happened to be curious about adding much smaller amounts of bovine gelatin (Mallinckrodt Chemicals, Type B, Cat. no: H219-59) to the solution of Table 1 and repeat the synthesis procedure (65 °C, 1 h) described in Chapter 2. The SEM image given in Fig. 4 shows the 120 nm-diameter monodisperse ACP nanospheres obtained by dissolving gelatin (67 mg L^{-1}) in the solution of Table 1 prior to syntheses. The BET surface area of these ACP spheres, which were recovered from their mother liquor by centrifugation, was 174 ± 23 m^2 g^{-1}. Ca/P molar ratio, Mg content (*via* ICP-AES analyses) and the XRD, FTIR, EDXS data of these gelatin-containing samples did not show any difference from the gelatin-free samples presented previously. Although we have thus shown that it would

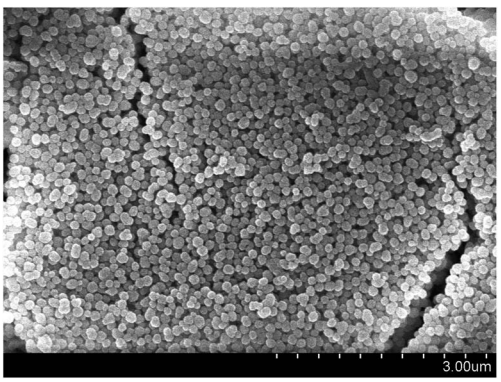

Fig. 4 FE-SEM image of ACP powders synthesized in a solution similar to that of Table 1 but containing 67 mg L^{-1} of gelatin in it (65 °C for 1 h).

be possible to decrease the mean diameter of ACP spheres using gelatin in the high ionic strength DMEM-like solution of this study, we still remain somewhat concerned about the possible *in vivo* toxicity of gelatin which may survive the routine precipitate washing procedures.[64,65]

4.6 Wettability of surfaces coated with ACP nanospheres

The high surface area and high wettability ACP produced by the solution presented here is promising for biomedical and pharmaceutical applications where altering the physicochemical properties of the surfaces of synthetic biomaterials becomes a necessity. Such surface alterations can be readily achieved by static (non-stirred) immersion of synthetic biomaterials (polymeric, metallic or ceramic) into this solution. The superb wettability of the nano-textured ACP deposited on the surface (as shown here for flat glass substrates) would be useful in attaching blood proteins more readily to the surfaces of blood-contacting biomaterials. As stated by Vroman,[66] on a surface, upon its contact with blood plasma, at least five proteins (*i.e.*, albumin, globulins, fibrinogen, fibronectin, and high molecular weight kininogen) displace each other in succession only within the first minute. Finally, the ACP spheres with diameters in the vicinity of 180 nm can also be used as non-cytotoxic and biocompatible drug delivery agents.

5 Conclusions

An aqueous solution, free of any organics, with identical HCO_3^-, Na^+, K^+, Mg^{2+}, Cl^- and phosphate ion concentrations to those of DMEM cell culture solutions was found to be able to deposit a 200 nm-thick monolayer of X-ray-amorphous calcium phosphate (ACP) at the physiological temperature of 37 °C, in less than 48 h, on glass slides vertically immersed in the solution. The ACP monolayer formed on glass slides was wetted by water at RT. The same solution was able to *in situ* form monodisperse nanospheres (having a mean diameter of 176 nm and a BET surface area of 185 $m^2 g^{-1}$) of X-ray-amorphous ACP when heated at 65 °C for 1 h under constant stirring. These two one-pot and simple synthesis processes mentioned above did not need any pH or ion concentration controls during the syntheses.

Notes

Certain commercial equipments, instruments, or chemicals are only identified in this article to foster understanding. Such identification does not imply recommendation or endorsement by the author, nor does it imply that the equipment or chemicals identified are necessarily the best available for the purpose.

Acknowledgements

The author gratefully acknowledges the generous help of Dr Preston L. Larson and Dr Andrew S. Madden of the University of Oklahoma for performing some of the SEM and XRD analyses of this study, when the author was a visiting professor at the College of Dentistry of the University of Oklahoma between 2010 and 2011. The author also thanks Dr Sharukh Khajotia of the University of Oklahoma College of Dentistry for letting us to use the contact angle goniometer of his laboratory.

References

1 M. L. Watson and R. A. Robinson, Collagen-Crystal Relationships in Bone. II Electron Microscope Study of Basic Calcium Phosphate Crystals, *Am. J. Anat.*, 1953, **93**, 25–59.
2 A. S. Posner, C. Fairy and C. J. Dallemagne, Defect Apatite Series in Synthetic and Natural Calcium Phosphates: The Concept of Pseudoapatites, *Biochim. Biophys. Acta*, 1954, **15**, 304–305.
3 E. D. Eanes, I. H. Gillessen and A. S. Posner, Intermediate States in the Precipitation of Hydroxyapatite, *Nature*, 1965, **208**, 365–367.
4 J. C. Weber, E. D. Eanes and R. J. Gerdes, Electron Microscope Study of Noncrystalline Calcium Phosphate, *Arch. Biochem. Biophys.*, 1967, **120**, 723–724.
5 J. D. Termine, R. A. Peckauskas and A. S. Posner, Calcium Phosphate Formation *In Vitro* II. Effects of Environment on Amorphous-Crystalline Transformation, *Arch. Biochem. Biophys.*, 1970, **140**, 318–325.
6 A. L. Boskey, Amorphous Calcium Phosphate: The Contention of Bone, *J. Dent. Res.*, 1997, **76**, 1433–1436.
7 F. Abbona and A. Baronnet, A XRD and TEM Study on the Transformation of Amorphous Calcium Phosphate in the Presence of Magnesium, *J. Cryst. Growth*, 1996, **165**, 98–105.
8 L. Brecevic, V. Hlady and H. Furedi-Milhofer, Influence of Gelatin on the Precipitation of Amorphous Calcium Phosphate, *Colloids Surf.*, 1987, **28**, 301–313.
9 J. Christoffersen, M. R. Christoffersen, W. Kibalczyc and F. A. Andersen, A Contribution to the Understanding of the Formation of Calcium Phosphates, *J. Cryst. Growth*, 1989, **94**, 767–777.
10 C. Combes and C. Rey, Amorphous Calcium Phosphates: Synthesis, Properties and Uses in Biomaterials, *Acta Biomater.*, 2010, **6**, 3362–3378.
11 S. Kim, H. S. Ryu, H. Shin, H. S. Jung and K. S. Hong, *In Situ* Observation of Hydroxyapatite Nanocrystal Formation from Amorphous Calcium Phosphate in Calcium-rich Solutions, *Mater. Chem. Phys.*, 2005, **91**, 500–506.
12 P. B. Y. Ofir, R. Govrin-Lippman, N. Garti and H. Furedi-Milhofer, The Influence of Polyelectrolytes on the Formation and Phase Transformation of Amorphous Calcium Phosphate, *Cryst. Growth Des.*, 2004, **4**, 177–183.
13 J. H. Tao, H. H. Pan, Y. W. Zeng, X. R. Xu and R. K. Tang, Roles of Amorphous Calcium Phosphate and Biological Additives in the Assembly of Hydroxyapatite Nanoparticles, *J. Phys. Chem. B*, 2007, **111**, 13410–13418.
14 H. H. Pan, X. Y. Liu, R. K. Tang and H. Y. Xu, Mystery of the Transformation from Amorphous Calcium Phosphate to Hydroxyapatite, *Chem. Commun.*, 2010, **46**, 7415–7417.
15 Z. Zyman, D. Rokhmistrov and V. Glushko, Structural Changes in Precipitates and Cell Model for the Conversion of Amorphous Calcium Phosphate to Hydroxyapatite

during the Initial Stage of Precipitation, *J. Cryst. Growth*, 2012, **353**, 5–11.
16 M. Kazanci, P. Fratzl, K. Klaushofer and E. P. Paschalis, Complementary Information on *In Vitro* Conversion of Amorphous (Precursor) Calcium Phosphate to Hydroxyapatite from Raman Microspectroscopy and Wide-Angle X-Ray Scattering, *Calcif. Tissue Int.*, 2006, **79**, 354–359.
17 N. C. Blumenthal, J. M. Holmes and A. S. Posner, Effect of Preparation Conditions on the Properties and Transformation of Amorphous Calcium Phosphate, *Mater. Res. Bull.*, 1972, **7**, 1181–1190.
18 J. L. Meyer and C. C. Weatherall, Amorphous to Crystalline Calcium Phosphate Transformation at Elevated pH, *J. Colloid Interface Sci.*, 1982, **89**, 257–267.
19 M. S. Tung and W. E. Brown, An Intermediate State in Hydrolysis of Amorphous Calcium Phosphate, *Calcif. Tissue Int.*, 1983, **35**, 783–790.
20 K. A. Gross and C. C. Berndt, Biomedical Applications of Apatites, in *Reviews in Mineralogy & Geochemistry*, Mineralogical Society of America, 2002, vol. 48, pp. 631–672.
21 D. D. Lee, C. Rey, M. Aiolova and A. Tofighi, Method of Preparing a Poorly Crystalline Calcium Phosphate and Methods of Its Use, US Pat., No. 7,517,539, 14 April 2009.
22 D. Knaack, M. E. P. Goad, M. Aiolova, C. Rey, A. Tofighi, P. Chakravarthy and D. D. Lee, Resorbable Calcium Phosphate Bone Substitute, *J. Biomed. Mater. Res., Part A*, 1998, **43**, 399–409.
23 S. Jalota, S. B. Bhaduri and A. C. Tas, A New Rhenanite (β-$NaCaPO_4$) and Hydroxyapatite Biphasic Biomaterial for Skeletal Repair, *J. Biomed. Mater. Res., Part B*, 2007, **80**, 304–316.
24 E. D. Eanes and J. L. Meyer, The Maturation of Crystalline Calcium Phosphates in Aqueous Suspensions at Physiologic pH, *Calcif. Tissue Res.*, 1977, **23**, 259–269.
25 S. V. Dorozhkin, Amorphous calcium (Ortho)phosphates, *Acta Biomater.*, 2010, **6**, 4457–4475.
26 D. Bayraktar and A. C. Tas, Chemical Preparation of Carbonated Calcium Hydroxyapatite Powders at 37 °C in Urea-Containing Synthetic Body Fluids, *J. Eur. Ceram. Soc.*, 1999, **19**, 2573–2579.
27 A. C. Tas, Synthesis of Biomimetic Ca-Hydroxyapatite Powders at 37 °C in Synthetic Body Fluids, *Biomaterials*, 2000, **21**, 1429–1438.
28 E. Landi, A. Tampieri, G. Celotti, R. Langenati, M. Sandri and S. Sprio, Nucleation of Biomimetic Apatite in Synthetic Body Fluids: Dense and Porous Scaffold Development, *Biomaterials*, 2005, **26**, 2835–2845.
29 F. Barrere, C. A. van Blitterswijk, K. de Groot and P. Layrolle, Influence of Ionic Strength and Carbonate on the Ca–P Coating formation from SBFx5 Solution, *Biomaterials*, 2002, **23**, 1921–1930.
30 T. Kokubo, H. Kushitani, S. Sakka, T. Kitsugi and T. Yamamuro, Solutions able to Reproduce *in vivo* Surface-Structure Changes in Bioactive Glass-ceramic A-W, *J. Biomed. Mater. Res.*, 1990, **24**, 721–734.
31 T. Kokubo and H. Takadama, How Useful is SBF in predicting *in vivo* Bone Bioactivity?, *Biomaterials*, 2006, **27**, 2907–2915.
32 W. R. Earle, E. L. Schilling, T. H. Stark, N. P. Straus, M. F. Brown and E. Shelton, Production of Malignancy *In Vitro*. IV. The Mouse Fibroblast Cultures and Changes Seen in the Living Cells, *J. Natl. Cancer Inst.*, 1943, **4**, 165–212.
33 J. H. Hanks and R. E. Wallace, Relation of Oxygen and Temperature in the Preservation of Tissues by Refrigeration, *Proc. Soc. Exp. Biol. Med.*, 1949, **71**, 196–200.
34 M. V. Tyrode, The Mode of Action of Some Purgative Salts, *Arch. Int. Pharmacodyn. Ther.*, 1910, **17**, 205–209.
35 H. A. Krebs and K. Henseleit, Untersuchungen ueber die Harnstoffbildung im Tierkoerper, *Hoppe-Seylers Z. Physiol. Chem.*, 1932, **210**, 33–66.
36 S. Ringer, Concerning the Influence Exerted by Each of the Constituents of the Blood on the Contraction of the Ventricle, *J. Physiol.*, 1882, **3**, 380–393.
37 D. Rohanova, A. R. Boccaccini, D. M. Yunos, D. Horkavcova, I. Brezovska and A. Helebrant, Tris Buffer in Simulated Body Fluid Distorts the Assessment of Glass-Ceramic Scaffold Bioactivity, *Acta Biomater.*, 2011, **7**, 2623–2630.
38 P. Premoli, A. Manzoni and C. Calzi, Method for the Quantitative Determination of Calcium in Biological Fluids through Direct Potentiometry, European Pat., no: EP 0153783 B1, 30 October 1991.
39 H. Eagle, Nutrition Needs of Mammalian Cells in Tissue Culture, *Science*, 1955, **122**, 501–504.
40 H. Eagle, Amino Acid Metabolism in Mammalian Cell Cultures, *Science*, 1959, **130**, 432–437.
41 R. Dulbecco and G. Freeman, Plaque Production by the Polyoma Virus, *Virology*, 1959, **8**, 396–397.
42 S. Mandel and A. C. Tas, Brushite ($CaHPO_4 \cdot 2H_2O$) to Octacalcium Phosphate ($Ca_8(HPO_4)_2(PO_4)_4 \cdot 5H_2O$) transformation in DMEM solutions at 36.5 °C, *Mater. Sci. Eng., C*, 2010, **30**, 245–254.
43 N. Temizel, G. Girisken and A. C. Tas, Accelerated Transformation of Brushite to Octacalcium Phosphate in New Biomineralization Media between 36.5° and 80 °C, *Mater. Sci. Eng., C*, 2011, **31**, 1136–1143.
44 R. Tadmor, Line Energy and the Relation between Advancing, Receding, and Young Contact Angles, *Langmuir*, 2004, **20**, 7659–7664.
45 M. R. Christoffersen, J. Christoffersen and W. Kibalczyc, Apparent Solubilities of Two Amorphous Calcium Phosphates and of Octacalcium Phosphate in the Temperature Range 30–42 °C, *J. Cryst. Growth*, 1990, **106**, 349–354.
46 P. C. H. Mitchell, S. F. Parker, K. Simkiss, J. Simmons and M. G Taylor, Hydrated Sites in Biogenic Amorphous Calcium Phosphates: An Infrared, Raman, and Inelastic Neutron Scattering Study, *J. Inorg. Biochem.*, 1996, **62**, 183–197.
47 A. C. Tas, Calcium Metal to Synthesize Amorphous or Cryptocrystalline Calcium Phosphates, *Mater. Sci. Eng., C*, 2012, **32**, 1097–1106.
48 E. Heyn, Short Reports from the Metallurgical Laboratory of the Royal Mechanical and Testing Institute of Charlottenburg, *Metallographist*, 1903, **5**, 37–64.

49 A. Oyane, K. Onuma, T. Kokubo and A. Ito, Clustering of Calcium Phosphate in the System $CaCl_2$–H_3PO_4–KCl–H_2O, *J. Phys. Chem. B*, 1999, **103**, 8230–8235.

50 E. D. Eanes, J. D. Termine and A. S. Posner, Amorphous Calcium Phosphate in Skeletal Tissues, *Clin. Orthop. Relat. Res.*, 1967, **53**, 223–235.

51 A. S. Posner and F. Betts, Synthetic Amorphous Calcium Phosphate and Its Relation to Bone Mineral Structure, *Acc. Chem. Res.*, 1975, **8**, 273–281.

52 A. Pasinli, M. Yuksel, E. Celik, S. Sener and A. C. Tas, A New Approach in Biomimetic Synthesis of Calcium Phosphate Coatings using Lactic Acid-Na Lactate buffered Body Fluid Solution, *Acta Biomater.*, 2010, **6**, 2282–2288.

53 M. A. Miller, M. R. Kendall, M. K. Jain, P. R. Larson, A. S. Madden and A. C. Tas, Testing of Brushite ($CaHPO_4 \cdot 2H_2O$) in Synthetic Biomineralization Solutions and *in situ* Crystallization of Brushite Micro-Granules, *J. Am. Ceram. Soc.*, 2012, **95**, 2178–2188.

54 National Oceanic and Atmospheric Administration (NOAA), http://www.ospo.noaa.gov/Products/ocean/sst/contour/index.html.

55 B. Alberts, A. Johnson, J. Lewis, M. Raff, K. Roberts and P. Walter, *Molecular Biology of The Cell*, Garland Science, New York, 2002.

56 X. Yin and M. J. Stott, Biological Calcium Phosphates and Posner's Cluster, *J. Chem. Phys.*, 2003, **118**, 3717–3723.

57 A. L. Boskey and A. S. Posner, Magnesium Stabilization of Amorphous Calcium Phosphate: A Kinetic Study, *Mater. Res. Bull.*, 1974, **9**, 907–916.

58 S. V. Dorozhkin, E. I. Dorozhkina and M. Epple, A Model System to Provide a Good *In Vitro* Simulation of Biological Mineralization, *Cryst. Growth Des.*, 2004, **4**, 389–395.

59 H. Zhou and S. Bhaduri, Novel Microwave Synthesis of Amorphous Calcium Phosphate Nanospheres, *J. Biomed. Mater. Res., Part B*, 2012, **100**, 1142–1150.

60 J. Sela, Bone Remodeling in Pathologic Conditions: A Scanning Electron Microscopic Study, *Calcif. Tissue Res.*, 1977, **23**, 229–234.

61 H. A. Lowenstam and S. Weiner, Transformation of Amorphous Calcium Phosphate to Crystalline Dahllite in the Radular Teeth of Chitons, *Science*, 1985, **227**, 51–53.

62 C. Holt and J. A. Carver, Darwinian Transformation of a 'Scarcely Nutritious Fluid' into Milk, *J. Evol. Biol.*, 2012, **25**, 1253–1263.

63 J. A. Arnesen and A. Gildberg, Preparation and Characterization of Gelatine from the Skin of Harp Seal (*Phoca groendlandica*), *Bioresour. Technol.*, 2002, **82**, 191–194.

64 F. S. Robscheit-Robbins, L. L. Miller and G. H. Whipple, Gelatin – Its Usefulness and Toxicity: Blood Protein Production Impaired by Continued Gelatin by Vein, *J. Exp. Med.*, 1944, **80**, 145–164.

65 M. Nahar, D. Mishra, V. Dubey and N. K. Jain, Development, Characterization, and Toxicity Evaluation of Amphotericin B-loaded Gelatin Nanoparticles, *J. Nanomed. Nanotechnol.*, 2008, **4**, 252–261.

66 L. Vroman, Finding Seconds Count after Contact with Blood (and That is All I Did), *Colloids Surf., B*, 2008, **62**, 1–4.

